J Therm Spray Tech (2018) 27:207–219
https://doi.org/10.1007/s11666-017-0669-8

PEER REVIEWED

Effect of Particle and Carbide Grain Sizes on a HVOAF WC-Co-Cr Coating for the Future Application on Internal Surfaces: Microstructure and Wear

J. Pulsford[1] · S. Kamnis[2] · J. Murray[1] · M. Bai[1] · T. Hussain[1]

Submitted: 1 August 2017 / in revised form: 17 November 2017 / Published online: 1 December 2017

Abstract The use of nanoscale WC grain or finer feedstock particles is a possible method of improving the performance of WC-Co-Cr coatings. Finer powders are being pursued for the development of coating internal surfaces, as less thermal energy is required to melt the finer powder compared to coarse powders, permitting spraying at smaller standoff distances. Three WC-10Co-4Cr coatings, with two different powder particle sizes and two different carbide grain sizes, were sprayed using a high velocity oxy-air fuel (HVOAF) thermal spray system developed by Castolin Eutectic-Monitor Coatings Ltd., UK. Powder and coating microstructures were characterized using XRD and SEM. Fracture toughness and dry sliding wear performance at three loads were investigated using a ball-on-disk tribometer with a WC-Co counterbody. It was found that the finer powder produced the coating with the highest microhardness, but its fracture toughness was reduced due to increased decarburization compared to the other powders. The sprayed nanostructured powder had the lowest microhardness and fracture toughness of all materials tested. Unlubricated sliding wear testing at the lowest load showed the nanostructured coating performed best; however, at the highest load this coating showed the highest specific wear rates with the other two powders performing to a similar, better standard.

Keywords ball-on-disk wear · HVOF · internal spray · WC-Co-Cr

This article is an invited paper selected from presentations at the 2017 International Thermal Spray Conference, held June 7-9, 2017, in Düsseldorf, Germany, that has been expanded from the original presentation.

✉ J. Pulsford
enxjcp@nottingham.ac.uk

T. Hussain
tanvir.hussain@nottingham.ac.uk

Introduction

In many engineering applications, wear is a life-limiting factor for various safety critical components, and one of the most extensively used types of wear-resistant coatings is industrial hard chromium or electrolytic hard chrome (EHC) [1]. However, due to the recent introduction of REACH (Registration, Evaluation, Authorization and Restriction of Chemicals), legislations regarding the use of

[1] Faculty of Engineering, University of Nottingham, Nottingham NG7 2RD, UK

[2] Castolin Eutectic-Monitor Coatings Ltd., North Shields NE29 8SE, UK

hexavalent chromium in the EU, the need for industry to replace this process has risen. High velocity oxy fuel (HVOF) thermal sprayed coatings are a deposition technology that can replace EHC coatings due to the fact that HVOF thermal spray coatings have better wear and corrosion performance and a lower life cycle cost [2]. WC-Co-Cr coatings have been chosen as a good potential material for this application, as this material displays wear resistance comparable to the widely used WC-Co but also offers an improvement in corrosion resistance. However HVOF processes are limited by their line of sight nature, meaning that spraying surfaces in tight confined areas is a challenge when compared to traditional EHC processes. Applying coatings on internal surfaces in tight spaces for complex geometries using most commercial HVOF systems is not feasible, due to the dimensions of the spray torch and the standoff distance required for optimal particle temperature and velocity; therefore, reducing the barrel length is necessary for operation in smaller geometries.

Internal diameter (ID) HVOF thermal spraying is a modern technology developed with the aim of mitigating these issues, operating at lower power levels but at the same time retaining high kinetic energy allowing a greater range of internal surfaces to be effectively coated. ID HVOF thermal spraying is a field that has been gaining the attention of researchers, with Lyphout and Björklund successfully applying a WC-Co-Cr coating with a powder particle size distribution of $-31 + 5.5$ µm on an internal surface of a pipe with a 200 mm ID using a newly developed ID HVAF (high velocity air fuel) system produced by UniqueCoat Technologies (Oilville, USA). The resulting coating had a hardness of 900 (HV0.3) and a porosity of approximately 1%, measured by image analysis of SEM images [3]. Although promising, these results show that the mechanical properties of these internally sprayed coatings are inferior to WC-Co-Cr coatings applied externally using current commercial high velocity oxy liquid fuel (HVOLF) spray technologies as these coatings have been shown to have a microhardness of over 1200 HV0.3 [4]. Therefore, further development is required before ID HVOF systems can compete with their externally sprayed equivalents.

As the temperature of the in-flight particles is strongly dependant on the length of the barrel, using conventional feedstock powders with a shorter barrel length may result in particle underheating, resulting in coatings with higher levels of porosity and lower hardness reducing the corrosion and wear resistance of the coating [5]. To mitigate these effects, powders with a reduced particle size range can be used as a smaller particle with a lower mass will accelerate at a faster rate, as well as requiring less energy to reach its optimum temperature when compared to larger, heavier particles of the same material. Along with this key advantage, spraying finer powder feedstocks has been previously shown to produce coatings with a lower porosity when compared to coarser-grained powders [6]. Alongside these materials, it has been reported that using nanostructured WC-Co-Cr feedstock powders results in coatings with better mechanical properties and sliding wear resistance than their coarse carbide grain counterparts, with Thakur and Arora producing a nanostructured WC-Co-Cr coating with a microhardness of 1646 HV0.3, compared to a coarse-grained coating which had a microhardness of 1147 HV0.3 [7]. Therefore, using either finer or nanostructured WC-Co-Cr powders may be a method to counter the lower power, barrel length and standoff distance present in ID HVOF thermal spray processes.

Although both finer and nanostructured WC-Co-Cr powder feedstocks have the potential to improve coating properties, both materials have been previously shown to be more vulnerable to decomposition of the WC phase. The mechanism for the decarburization in WC-based cermet coatings has been studied, and it has been shown that carbon loss occurs as follows. The binder phase melts before the WC phase, due to its lower melting point. At this point, WC will begin to dissolve into the molten binder, after which carbon will begin to be removed by the solution by reacting with oxygen at the gas–liquid interface. On impact with the substrate, the solution is rapidly quenched and the binder phase solution becomes supersaturated, resulting in the release of W_2C [8]. Simultaneously, the formation of an amorphous or nanocrystalline supersaturated solid cobalt, tungsten carbide solution or η phase carbide can also take place, meaning a binder phase of varying compositions may be observed throughout the microstructure [9]. As finer particles are more susceptible to overheating due to their lower mass and nanoscale WC grains may dissolve more readily in the molten binder due to their higher surface area-to-volume ratio compared to coarse WC grains, the likelihood of decarburization occurring by the above mechanism increases when spraying finer or nanostructured powders. Therefore, when using these materials the optimization of spray parameters is the key to producing a coating with a high density of the WC phase.

In this study, a HVOAF (high velocity oxy-air fuel) spray system capable of operating with a mixture of air and organic fuel gases developed by Castolin Eutectic-Monitor Coatings Ltd. (North Shields, UK) was used to spray three separate WC-Co-Cr powders with the same composition but differing powder particle size ranges and carbide grain sizes. The microstructures and the associated mechanical properties were studied. Unlubricated sliding wear testing against WC-Co counterbody was used to study the effect of powder particle size range or carbide size on the coating's sliding wear resistance and as a means to test the performance of the three coatings.

Experimental Methods

Feedstock Materials

Three separate commercial WC-Co-Cr powders (H.C. Starck Ltd., Munich, Germany) with the same composition (WC—10% Co—4% Cr in wt.%) but differing carbide grain sizes and powder particle size distributions were used in this study. The details of the powders are displayed in Table 1; the MC-30 and MC-15 powders are stated by the manufacturer to have a medium WC grain size, but differ in powder particle size range. The third feedstock powder NC-30, meanwhile, has a nanoscale WC grain size, therefore meaning that the effect of WC grain size and powder particle size range on the coating microstructure, mechanical properties and wear resistance can be compared.

HVOAF Coating Deposition

All coatings were deposited onto 38.1 mm diameter x 6 mm disks of EN 1.4401 grade 316 stainless steel (16% Cr, 10% Ni and 2% Mo, in wt.%) for characterization and wear testing using a next-generation HVOAF system capable of depositing coatings on internal surfaces developed by Castolin Eutectic-Monitor Coatings Ltd. [10]. This system uses an isentropic cone-shaped nozzle to accelerate the combustion gases to supersonic velocities reaching Mach 2.7 [11]. Prior to coating deposition, all substrate materials used were cleaned and grit blasted to maximize particle–substrate bonding. The spray parameters used in this study were chosen based on data from previous optimization studies. The torch uses air (60-500 SLPM) and O_2 (50-170 SLPM) depending on the mode of operation, aiming for 100% stoichiometric combustion.

Dry Sliding Wear Testing

Unlubricated sliding wear tests were carried out at room temperature ($\approx$ 25 °C, relative humidity $\approx$ 60%) using a rotating ball-on-disk tribometer against a 94% WC—6% Co ball with a diameter of 9.5 mm (Dejay Distribution Ltd., Launceston, UK) that was replaced at the end of each test. The details of the sliding wear rig are described elsewhere [12]. The experimental parameters used during the sliding wear tests were selected with the aim of simulating typical conditions for components in the aerospace industry that experience sliding wear. Uninterrupted wear tests were run at loads of 96, 168, and 240 N with a sliding distance of 500 m and sliding speed of 0.05 m/s. These three loads were selected in order to simulate the low-, medium- and high-load environment to determine if the coatings experience a different wear regime as conditions are changed. Prior to the wear test, the top surface of the coatings was grinded and polished down to a 1 µm finish. Both the coating sample and the ball counterbody were cleaned with IMS before and after testing.

The volume loss of each disk was determined using the profilometry method used in a number of other studies [13, 14]; a surface profiler (Taylor Hobson Ltd., Leicester, UK) was used to measure four line traces perpendicular to the sliding direction, and from each of these the cross-sectional area of material loss could be determined. These were averaged and multiplied by the total track length to calculate the total volume of material lost. The specific wear rate could then be calculated by dividing the total volume of material lost by the product of the total distance slid and the load used. The wear of the WC-Co ball resulted in a near flat surface and using the assumption that this represented the removal of a spherical cap of material, and Eq 1 and 2 can be used to calculate the volume loss of the counterbody [15]:

$$d = r - \sqrt{(r^2 - a^2)} \quad \text{(Eq 1)}$$

$$\Delta V = \pi d^2 \left(r - \frac{d}{3} \right) \quad \text{(Eq 2)}$$

where ΔV represents the volume loss, r the ball radius, and a the radius of the wear scar.

The morphology of the wear scar and fracture mechanisms were then examined in plain view using a scanning electron microscope (Jeol 6490LV, Jeol Ltd., Japan), with optical microscopy (Nikon Eclipse LV100ND, Nikon, Japan) used to image the WC-Co counterbody.

Coating Characterization

X-ray diffraction (XRD) was performed on the feedstock powders and as-sprayed coatings using a Siemens D500 with Cu $K\alpha$ radiation (1.5406 Å) in the $20° \leq 2\theta \leq 90°$ range to identify the phases present in the powders and coatings. A step size of 0.02° and dwell time of 3 s was

Table 1 Method of manufacture, nominal size distribution and carbide grain size of the feedstock powders

Commercial designation	Powder code	Processing method	Powder size, µm	Carbide grain size
AMPERIT® 557.059	MC-30	Agglomerated and sintered	− 30 + 5	Medium (1-2 µm)
AMPERIT® 507.059	NC-30	Agglomerated and sintered	− 30 + 5	Nanometric (200-400 nm)
AMPERIT® 554.067	MC-15	Sintered and crushed	− 15 + 5	Medium (1-2 µm)

used. Sections of the coating were cut from the bulk sample using a diamond tipped precision cutting wheel; powder and coating cross sections were then obtained by mounting in a conductive mounting compound (Metprep Ltd., UK), ground with SiC papers down to 15.3-µm grit finish, and then finally were polished down to a 1-µm finish.

The powder morphologies and coating microstructures were imaged using SEM (JEOL 6490LV, JEOL Ltd., Japan) operated in high vacuum mode and utilizing both secondary electron imaging (SE) and backscattered electron imaging (BSE). The carbide grain size of the feedstock powders, coating thickness and coating porosity were measured using image analysis software to process a collage of five SE SEM images (Image J, National Institute of Health, USA). Each image used for the porosity measurement covered an area of coating approximately 420 µm in length and 270 µm in height, meaning the porosity measurement of each coating was determined by analyzing approximately along 2.1 mm of the coating length, or 0.6 mm^2 of the coating cross section.

The microhardness of the coatings was measured on polished cross sections by using a Vickers microhardness indenter (Buehler, Illinois, USA) at a load of 300 gf and a dwell time of 10 s; for each sample, 6 indentations were made in the center of the coatings running parallel with the substrate. Fracture toughness of the coatings was measured by indenting on polished cross sections with a 2.5 kgf load and measuring the crack lengths parallel to the substrate using optical microscopy; cracks propagating from the left and right tips of the indent were considered. The fracture toughness K_c was determined using the method described by Evans and Wilshaw [16], shown in Eq 3:

$$K_c = 0.079\left(\frac{P}{a^{3/2}}\right)\log\left(\frac{4.5a}{c}\right) \quad \text{(Eq 3)}$$

where P is the applied indentation load, a is the indentation half diagonal, and c is the crack length from the indent center. This expression is only valid when $0.6 \leq c/a \leq 4.5$; all measurements of c and a were determined to fit within this range.

Results

Feedstock Powder Characterization

SEM micrographs (Fig. 1) show that the MC-30 and NC-30 powders both exhibit a spherical structure with some porosity; cross-sectional images of these powders show that this porosity is also present within the inner structure of the powder particles. The SE images of the NC-30 powder show a much more compact morphology than those of the MC-30 powders, suggesting that even the actual surface area of the MC-30 powder particles may be larger than the NC-30 powder particles.

The MC-15 powder was observed to have a blocky, angular morphology with a lower visible porosity both internally and externally; this difference was attributed to the different methods of powder manufacture used (MC-15 was sintered and crushed, while the other two powders were agglomerated and sintered). The powders with the medium WC grain size MC-30 and MC-15, and the nanostructured powder NC-30 were found to have a carbide grain size between 1-2 µm and 200-400 nm, respectively.

The XRD spectra in Fig. 2 show that some differences in the phase composition between the three powders exist. Aside from the primary WC and Co. fcc phases, additional phases were detected within the MC-30 and MC-15 powders, with the diffraction peaks indicating that these include the η-phase (W, Co, Cr) $_6$C or (W, Co, Cr)$_7$C$_3$ as seen by other researchers [4]. However, these two phases are difficult to distinguish in XRD analysis due to the fact that the two main diffraction peaks for these phases are very close to one another, with peaks of the η-phase and (W, Co, Cr)$_7$C$_3$ being located at 2θ values of 42.4° and 42.5°, respectively. It can be observed that a degree of shifting of these peaks has occurred in the MC-15 powder, possibly indicating that W or Co has dissolved into the (W, Co, Cr)$_7$C$_3$ phase, substituting itself for Cr in the lattice [4].

Coating Microstructure and Mechanical Properties

Low-magnification images (see Fig. 3) of the coatings show that all three coatings display a macroscopically dense structure, with no large pores visible and no crack or delamination at the coating–substrate interface. The coating thickness (see Table 2) can be seen to vary between the coatings, with the nanostructured coating being considerably thicker. Porosity in all three coatings is very low, with the MC-30 coating having the highest at a level of approximately 0.53 ± 0.24% and the coating sprayed with the finer powder MC-15 having the lowest at approximately 0.27 ± 0.11%. BSE images (Fig. 3) show the microstructures of the coatings. The MC-30 and MC-15 coatings both exhibit a very similar microstructure; WC grains with irregular shape and size are surrounded by a metallic binder phase of varying composition. Areas of the binder phase showing a brighter contrast indicate regions in which the WC grains have dissolved into the matrix, with the brighter contrast being the result of increased tungsten levels. Some of the WC grains residing in these W heavy binder zones were observed to be surrounded by a "halo" of another phase displaying an even brighter contrast, which has been confirmed by other researchers as being W_2C [9]. This feature can be seen in larger numbers in the

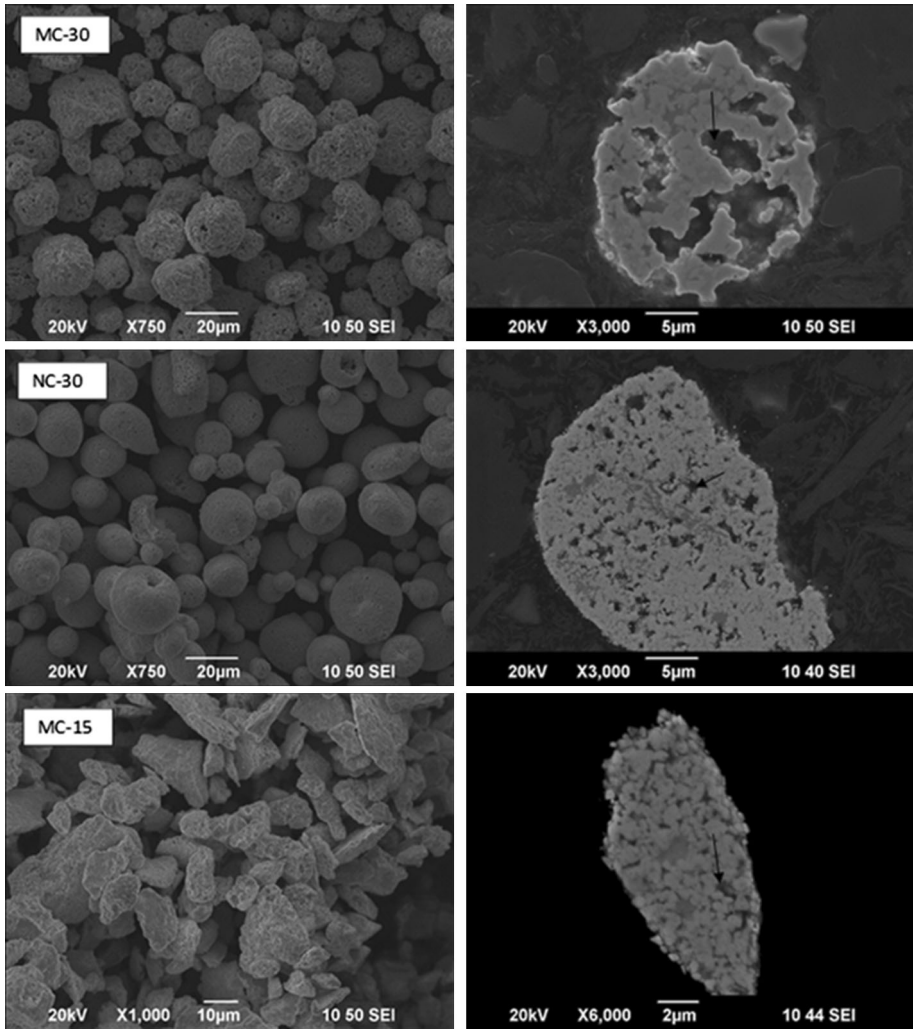

Fig. 1 SEM images of the three powders. The spherical shape of the MC-30 and NC-30 powders can be observed, with internal porosity visible in all three powders (marked with an arrow)

MC-15 coating, indicating that the finer powder decarburized more during the spray process; this result is confirmed by the XRD spectra in Fig. 2. Alongside these phases, other areas of the binder phase exhibit a much darker contrast in both the MC-30 and MC-15 coatings; these areas are not porosity but have been shown by EDX analysis to be a Cr- and O-rich phase with a lower W composition in comparison with other areas of the binder.

The NC-30 coating was found to have a different microstructure compared to the other two coatings; due to the much smaller size of the WC grains, they dissolve more readily in the binder during the spray process, resulting in areas of tungsten heavy binder in which the individual WC grains can no longer be seen due to dissolution. Small spots observed on the image of an even brighter phase can be seen in some of these areas which indicate the presence of W_2C. The presence of the dark Cr-rich phase seen in the other two coatings was found to still be present in the NC-30 coating; however, this phase was found to be less common in the nanostructured coating.

The diffraction patterns given by XRD in Fig. 2 indicate that W_2C has formed in all three coatings; therefore, supplementing the SEM images and confirming that different degrees of decarburization have occurred in all three coatings. The height of the W_2C peaks in relation to the WC peaks is significantly larger for the MC-15 coating, giving more evidence for increased decarburization compared to the other two coatings, in which the levels of W_2C appear to be quite similar. The index of carbon retention, a ratio of the peak heights between the (1 0 0) peak of WC at $2\theta = 35.6°$ and (1 0 1) peak of W_2C at $2\theta = 39.6°$ was calculated for the three coatings using the method shown in other work [17]. The results are shown in Table 2, which show that less carbon was retained in the MC-15 coating in comparison with the other two, meaning that decarburization was more severe when spraying this material with the selected parameters. All three coatings show no detected peaks of the Co fcc, η-phase and M_7C_3 phases that were found with the powder feedstocks.

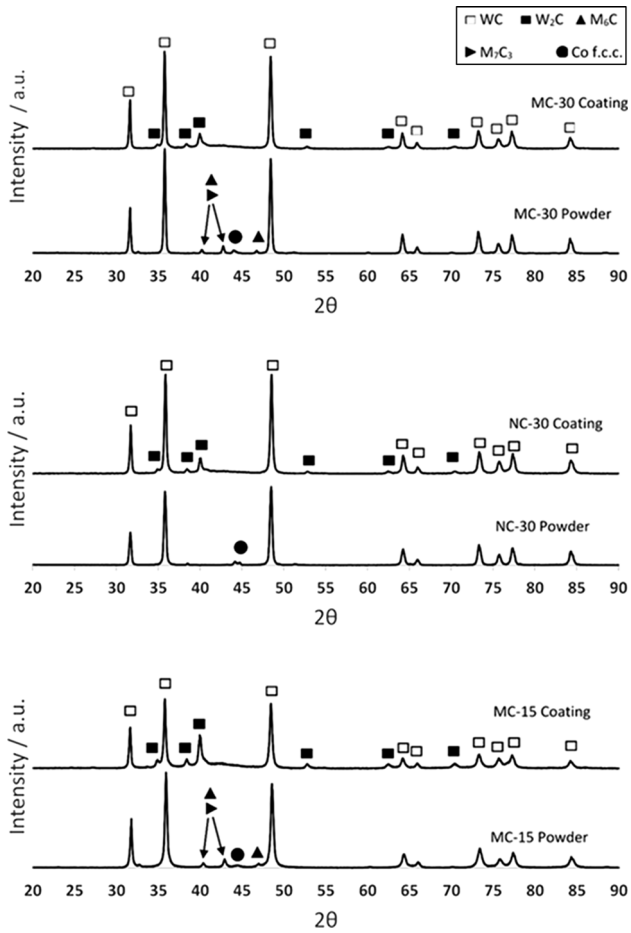

Fig. 2 XRD spectra of each feedstock powder and its corresponding coating. Note the larger W2C peak for the MC-15 coating

Mechanical properties of the three coatings are shown in Table 2; the microhardness of the MC-30 and MC-15 coatings was found to be at similar levels. The nanostructured NC-30 coating was found to have the worst mechanical properties of the three coatings tested, with the lowest microhardness and fracture toughness at values of 1246 ± 58 and 3.62 ± 0.65 MPa $m^{0.5}$, respectively.

Dry Sliding Wear Test

The specific wear rates of the coatings and WC-Co counterbodies at the three loads used during the sliding wear testing are shown in Fig. 4, 5, and 6. The MC-30 coating (Fig. 4) was shown to perform similarly across the three loads tested, with the increased load only resulting in heightened counterbody wear; this may suggest that the same mechanism of wear is taking place at all loads tested. Although similar specific wear rates were measured for the MC-15 coating (Fig. 6) at 96 and 240 N, a slight increase was seen at 168 N. This, however, is balanced out by reduced counterbody wear at this load, meaning the MC-15 coating wore out more aggressively in relation to the counterbody in comparison with the other coatings at 168 N. The NC-30 coating (Fig. 5) displayed a different trend in comparison with the other two coatings; the specific wear rate was almost an order of magnitude lower than the others at 96 N, but with heightened load a large increase in wear was observed resulting in this coating performing the worst at 240 N. This difference in performance in comparison with the other coatings across the three loads may suggest that a separate wear mechanism is taking place in the nanostructured coating or that the inferior mechanical properties of this coating mean it suffers more greatly at higher load.

The counterbody wear rates were an order of magnitude higher than those measured for the coatings. As the load was raised, the specific wear rate of the WC-Co counterbodies used with the MC-30 and MC-15 coatings increased at a larger rate than the coating specific wear rates, suggesting that counterbody wear is more susceptible to increased load than the coating wear with these two coatings. For the nanostructured NC-30 coating, the specific wear rate of the counterbody increased at a similar rate to the coating wear with elevated load.

Top Surface Analysis of the Wear Samples

To gain an understanding of the wear mechanisms taking place, the plan view of the wear tracks was analyzed using SEM. Figure 7 shows the worn surfaces of the three coatings tested at the 96 N load. Sections of material can be seen appearing to crack and break off from the coating surface in the MC-30 and MC-15 coatings, and at higher magnification, it can be observed that these sections breaking off consist of a different phase, and this is labeled in Fig. 7 with an arrow. EDX analysis showed that the composition of this phase consists primarily of tungsten and oxygen (W = 64.65 wt.%, O = 26.40 wt.%), suggesting that this phase is an oxidized particle formed due to the work done on the coating surface by the counterbody being converted to heat energy, resulting in localized higher temperatures on the coating surface and therefore increasing the oxidation rate (tribo-oxidation). However, this phase was found to form much less significantly on the NC-30 coating when tested at 96 N which may explain the lower specific wear rate recorded. On this coating, the primary source of wear appears to be from scratches running in the direction of counterbody movement, suggesting plowing has taken place with the abrasive body probably consisting of WC particles, as these would have sufficient hardness to cause abrasion on the soft binder phase. Areas in which pullout of the carbide grains can be detected, suggesting that these abrasive particles probably originated from the coating surface.

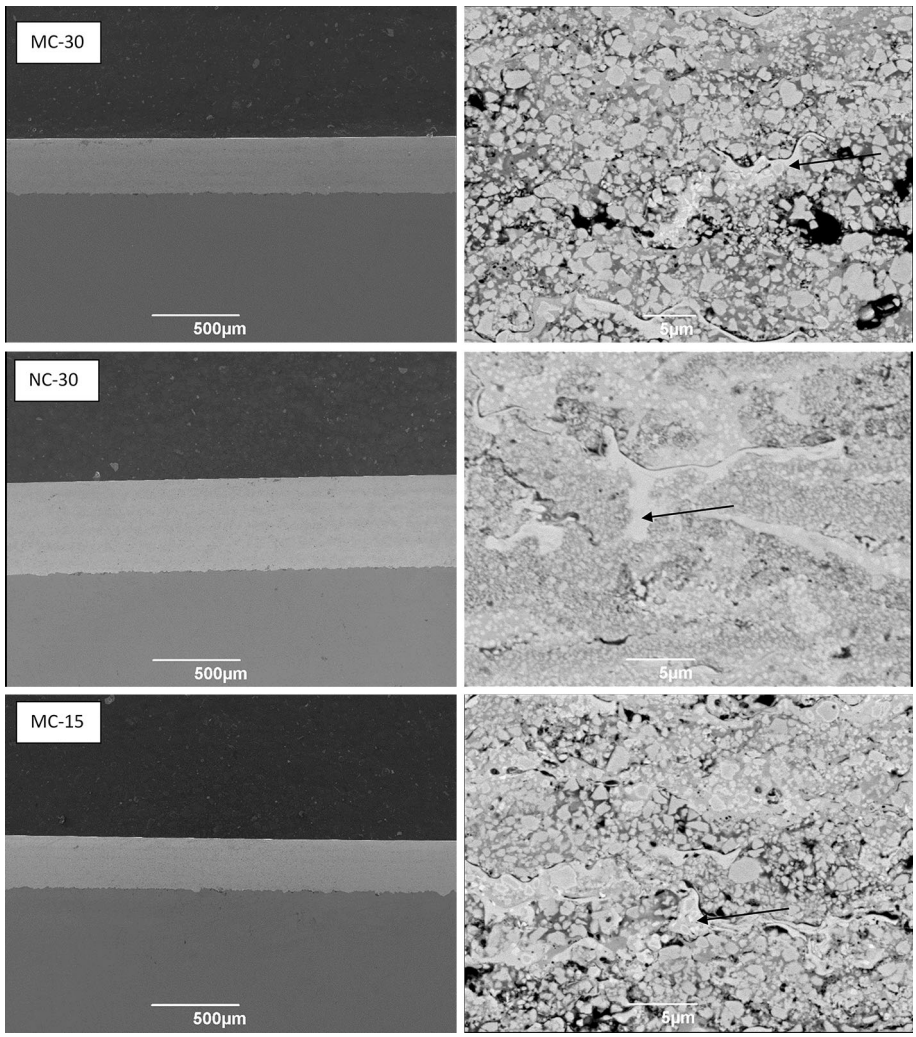

Fig. 3 Left: low magnification SE SEM images of the coating cross section. Right: BSE SEM images of coating cross section microstructure. Example areas of W heavy binder are labeled with arrows. Areas with a black contrast were found to not be porosity, but a Cr-rich phase

Table 2 Summary of coating properties

Sample name	Coating thickness, µm	Microhardness (HV0.3)	Fracture toughness Kc, MPa $m^{0.5}$	Porosity, %	Index of carbon retention
MC-30	317	1313 ± 60	4.00 ± 0.36	0.53 ± 0.24	0.86
NC-30	512	1246 ± 58	3.62 ± 0.65	0.34 ± 0.15	0.85
MC-15	290	1341 ± 43	3.89 ± 0.52	0.27 ± 0.11	0.67

Figure 8 shows the worn coating surfaces when the load is increased to 168 N; on all three coatings, the presence of the oxidized particles with cracks can be observed. This was observed in particular on the MC-15 coating, which was measured to have the highest specific wear rate at this particular load suggesting that the formation of this layer of oxidized particles has a significant impact on the measured specific wear rate. Signs of abrasive wear can be observed particularly on the MC-30 and NC-30 coatings in the form of scratches in the direction of the counterbody movement, probably the result of a similar abrasion mechanism occurring with WC particles acting as the hard phase, as is previously described above for the NC-30 coating at 96 N.

The worn surfaces of the coatings tested at 240 N are displayed in Fig. 9. The formation of the cracked oxidized particles is observed on all three coatings, especially again on the MC-30 and MC-15 coatings. It can be seen that the width of the wear track is larger on the NC-30 coating in comparison with the other two coatings which may explain why this coating had the highest measured specific wear rate.

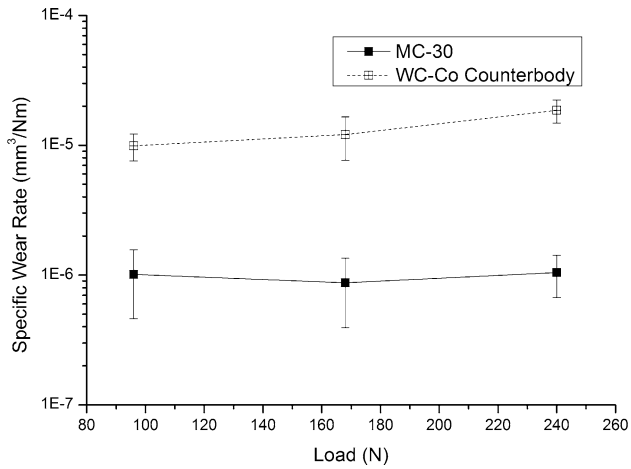

Fig. 4 Specific wear rates of the MC-30 coating and associated counterbody at 96, 168, and 240 N

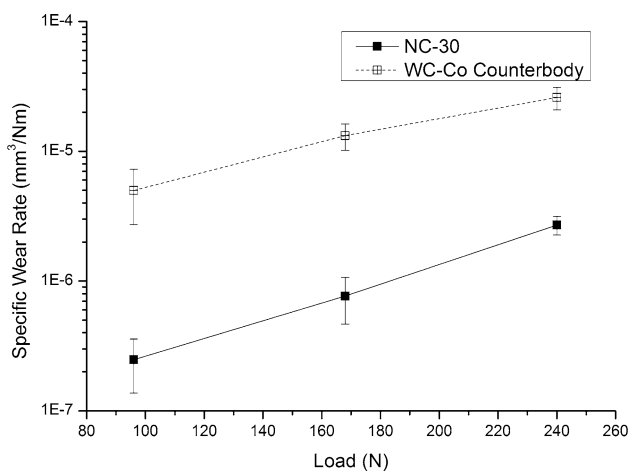

Fig. 5 Specific wear rates of the NC-30 coating and associated counterbody at 96, 168, and 240 N

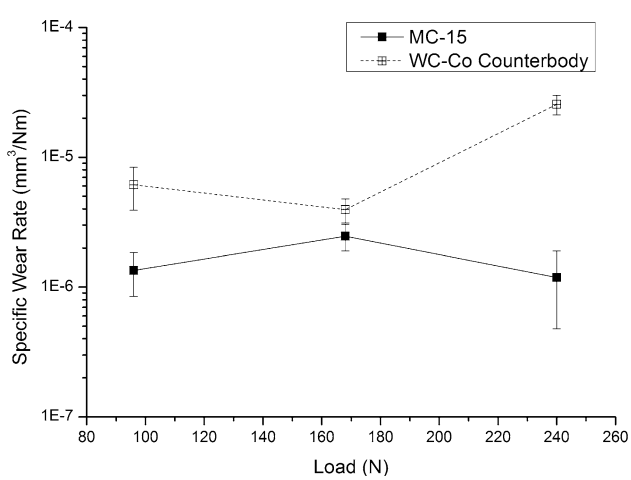

Fig. 6 Specific wear rates of the MC-15 coating and associated counterbody at 96, 168, and 240 N

Discussion

Coating Microstructure and Mechanical Properties

All three powders suffer from some degree of decarburization when being sprayed with this HVOAF spray system at the selected spray parameters, which is the expected result when comparing this data to previous work as WC cermet powders have been shown to suffer carbon loss when exposed to the high temperatures present in the HVOF process [18, 19]. In particular, the finer powder MC-15 was found to decarburize more significantly than the other powders; this is probably due to the higher temperatures reached by the smaller powder particles during spraying when compared to the other powders, resulting in increased WC dissolution in the metallic binder.

In contrast to other findings [20], it was found that the nanostructured powder NC-30 decarburized at a similar rate to the larger WC grain MC-30 powder. It is previously described that when following the established mechanism for the carbon loss in WC cermet coatings, the nanostructured coating should be expected to decarburize at a greater rate due to the increased surface area-to-volume ratio of the smaller WC grains leading to higher dissolution of these grains in the binder phase during spraying. This effect, however, may have been counteracted by the fact that the MC-30 powder particles appear to possess a less compact morphology than the NC-30 powders, meaning that the actual surface area may be lower on the nanostructured powder. A reduced surface area results in a smaller heat transfer area, reducing decarburization and therefore possibly explaining why these two powders were similar in terms of decarburization. However, as the surface area of the particles was not explicitly measured, this cannot be verified for certain.

The results of the current study indicate that powder particle size has a much larger effect on decarburization than carbide size, suggesting that particle temperature is the most important factor affecting carbon loss when applying these coatings using this spray system. This could be due to two possible factors; the heightened decarburization at increased particle temperatures may be due to increased solubility of the liquid binder or increased liquid fraction of the binder phase at the higher temperature leading to greater dissolution of the WC grains. It is possible that carrying out further spray parameter optimization work to suppress the melting of the metallic binder phase could inhibit the dissolution of the WC phase, meaning that the performance of the coatings in this study could be improved further in time.

Previous researchers have stated that nanostructured WC-Co-Cr powder feedstocks result in coatings with a

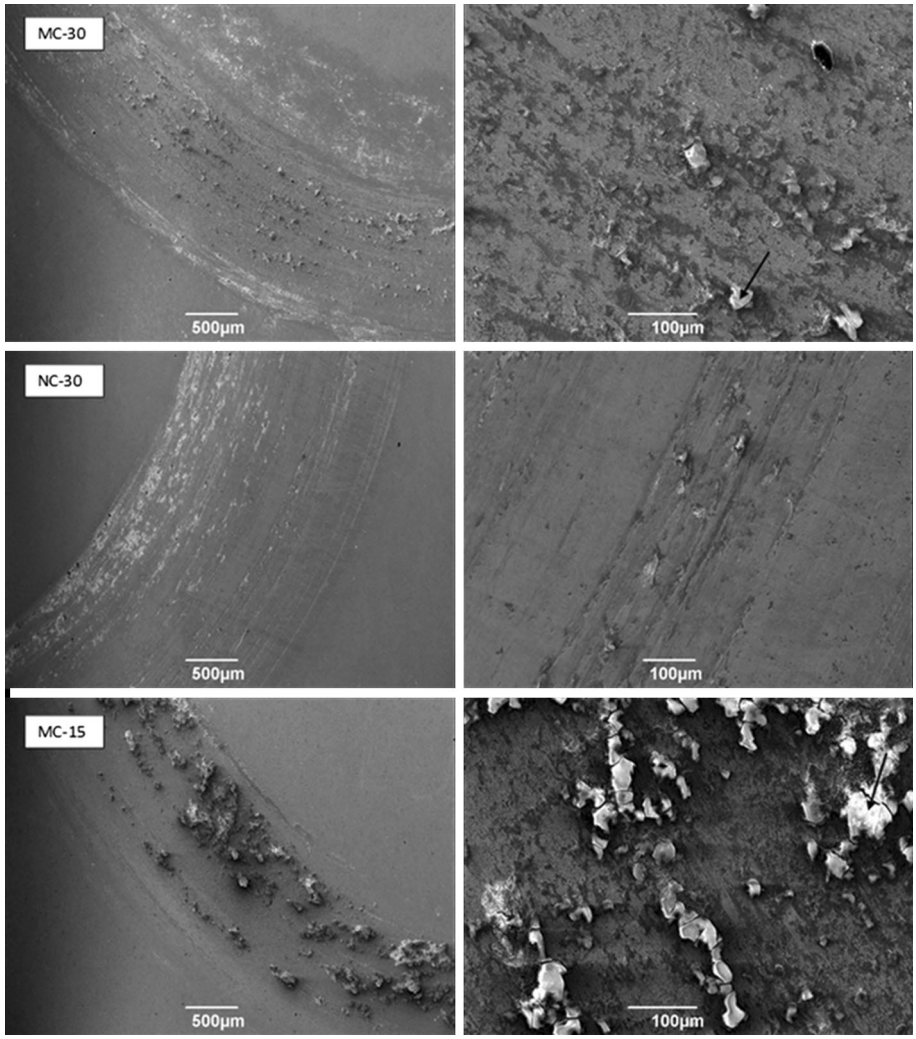

Fig. 7 Left: lower magnification SE SEM images of the worn surfaces of the three coatings at 96 N. Right: higher magnification top-down SE images of the worn surfaces. A brittle phase can be observed on the coating surfaces, most notably on the MC-30 and MC-15 coatings, and is marked on the images

much higher hardness; their reasoning being that reducing the carbide size results in increased hardness and fracture toughness due to the Hall–Petch effect [7]. This is because decreasing the carbide grain size and binder mean free path results in increased suppression of dislocation propagation and this jamming of slip therefore means fracture toughness is increased [21]. However, the results of this study may differ from these statements, with the nanostructured coating NC-30 being shown to possibly have a slightly lower microhardness and fracture toughness than the other two coatings.

It was determined that the MC-30 and MC-15 coatings had a similar microhardness level. Previous studies carried out using this spray system determined that higher in-flight particle velocities result in greater cold hardening effects, due to the increased peening effect on the substrate [11]. This effect may lead to resulting increased compressive residual stresses in the MC-15 coating when compared to MC-30, leading to an overall increase in microhardness. This hardening effect, however, is counteracted in the MC-15 coating by the increased level of WC dissolution taking place, meaning the resulting microhardness of the two coatings is at a similar level.

Another possible factor affecting the microhardness and fracture toughness of the three coatings is the amount of W_2C present in the coating microstructure. It has been previously shown that the microhardness of cast WC and W_2C is 17,000 and 30,000 MPa, respectively [22], suggesting that the formation of W_2C due to decarburization could result in an increase in coating microhardness. This result has also been suggested in a number of other studies [23, 24]. However, the elevated presence of W_2C may also reduce the fracture toughness of the coating, with the fracture toughness of WC and W_2C being measured at 5.9 and 3.6 MPa $m^{1/2}$, respectively [25]. The results in this study appear to agree with this hypothesis, especially when studying the MC-30 and MC-15 coatings, as the reduced fracture toughness of the MC-15 coating could be explained by the increased presence of W_2C.

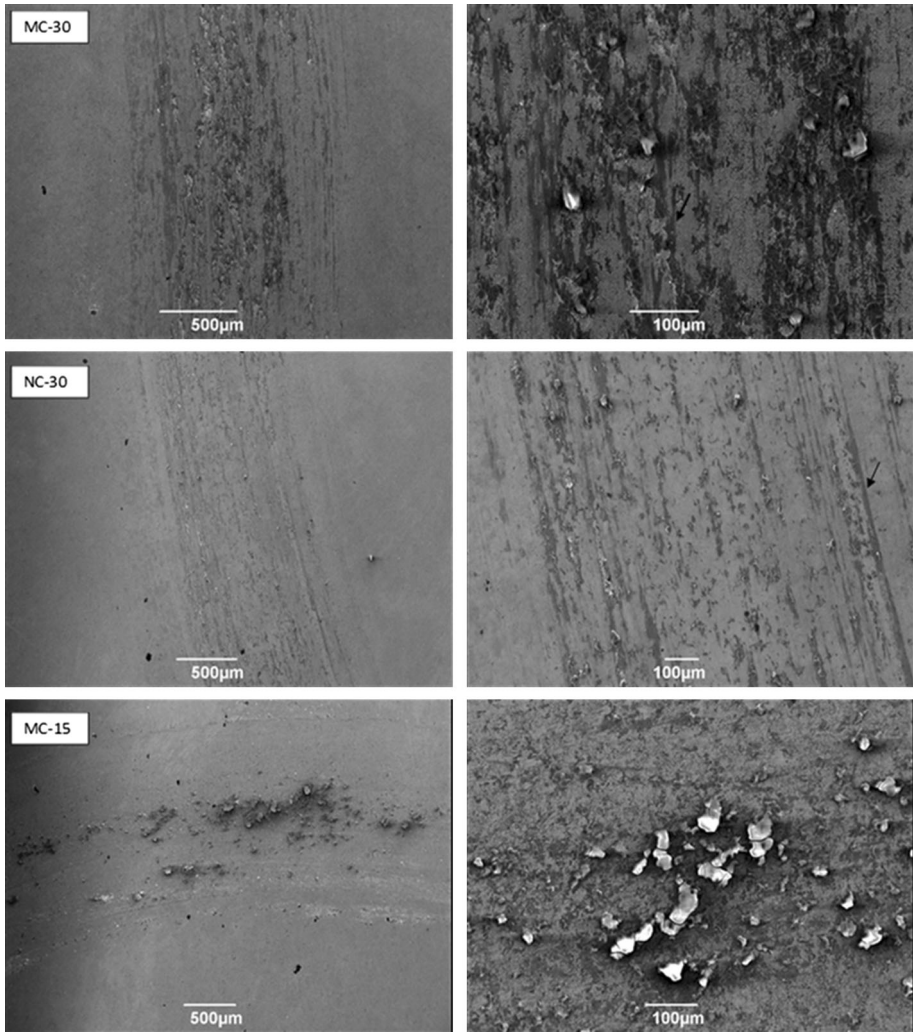

Fig. 8 Left: lower magnification SE SEM images of the worn surfaces of the three coatings at 168 N. Right: higher magnification top-down SE images of the worn surfaces. Scratches due to abrasion from wear debris are marked

Increased porosity has been shown to reduce the microhardness of coatings [26], and as the measured porosity was higher in the MC-30 coating than the MC-15 coating, this may also have an effect. The nanostructured coating displayed a lower amount of W_2C than the MC-15 coating, but had reduced microhardness and fracture toughness suggesting that reducing the WC grain size has an overall negative effect on the coating's mechanical properties when spraying using the novel HVOAF torch utilized in this study.

Powder particle size has also been shown to affect coating porosity, as the percentage porosity of the MC-30 powder is almost double that of the MC-15 powder. This could again indicate that the in-flight velocity of the particles when spraying the MC-15 powder is higher than the others, as it has been shown previously that reaching a greater particle velocity during spraying leads to reduced porosity in the final coating [5]. In addition, it has also been shown that coating porosity is reduced as coating thickness is increased [27], meaning that the reduced porosity could be due to the higher thickness of the NC-30 coating.

Wear Behavior

Past studies have often concluded that decarburization of WC cermet coatings has a negative effect on the sliding wear resistance of the coatings as the presence of hard but brittle W_2C has been said to reduce toughness and increase wear [28].

At 96 N, the nanostructured coating performed best, showing wear rates significantly lower than the other two coatings. Meanwhile, at this load and at 168 N the MC-15 coating, which was found to have suffered the most carbon loss (Fig 2), displayed the highest specific wear rates seemingly in agreement with the above statement (Fig 6). However, as the load was increased to 240 N, this coating was found to perform similar to previous two loads but better than the nanostructured coating. This suggests that

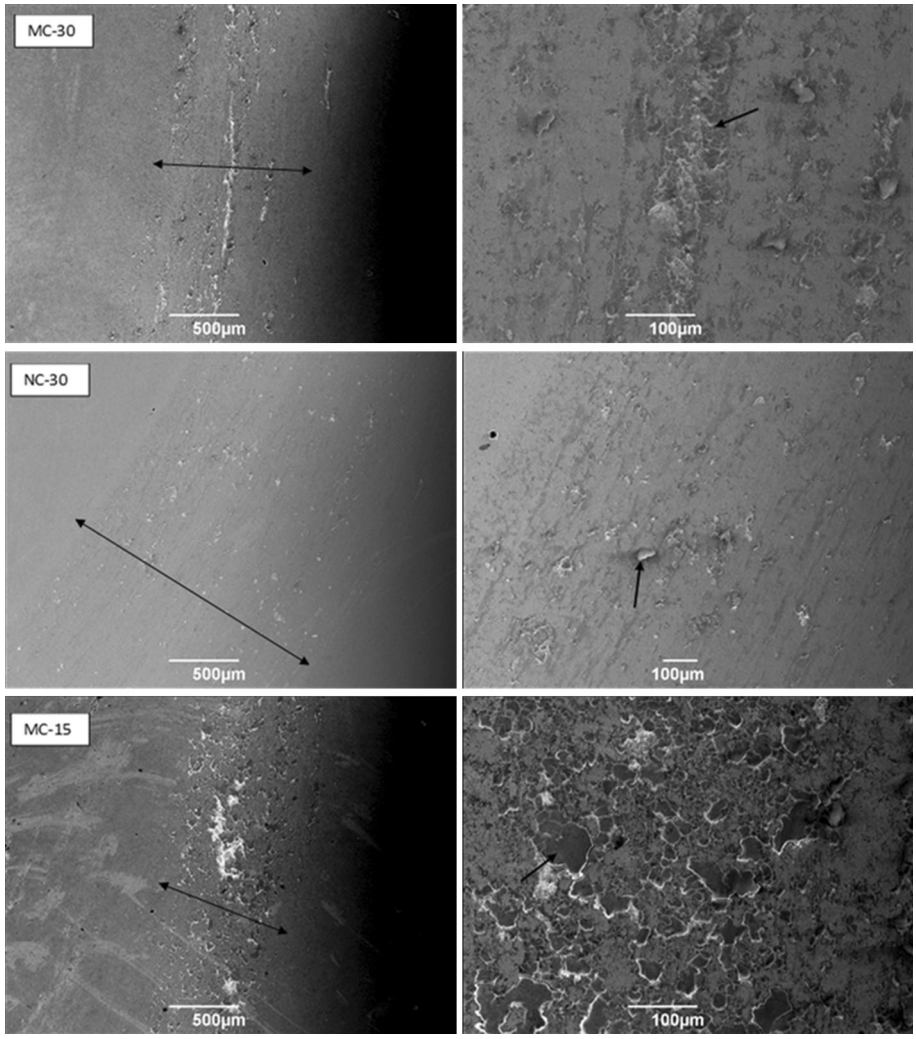

Fig. 9 Left: lower magnification SE SEM images of the worn surfaces of the three coatings at 240 N. Right: higher magnification top-down SE images of the worn surfaces

the inferior microhardness and fracture toughness of the NC-30 coating resulted in it suffering more under the higher load in comparison with the other two coatings, making it suffer the highest amount of wear at 240 N.

The width of the wear track was shown to be significantly larger on the NC-30 coating when tested at 240 N, in comparison with the other two samples tested, meaning that although the normal force exerted on each coating is equal, the pressure is not. This effect could explain the reduced number of oxidized particles on the surface of the wear track for the NC-30 coating at 240 N, as the normal force is exerted onto a larger area due to the wider wear track, meaning that the frictional forces are less concentrated, meaning less tribo-oxidation takes place.

As the trend of the NC-30 coating wear differs greatly from the other two larger WC grained coatings, it is likely that a different mechanism of wear is taking place with this coating. At the 96 N load, the oxidized particles that can be observed on the surface of the wear tracks on the MC-30 and MC-15 coatings in Fig. 7 did not form nearly as significantly on the NC-30 coating. This could possibly indicate lower frictional forces and therefore less heat energy available for the film formation to take place, and this could explain why the nanostructured coating performed better than the others at 96 N, making this coating possibly more suitable than the others for applications where protection from smaller loads is required. However, the inferior microhardness and fracture toughness of this coating may have been the reason for the worse performance of this coating at the 240 N load.

Future Application of a WC-Co-Cr Coating for Internal Surfaces

When coating internal diameters, the local environment in which the spray torch is operating is very different; the standoff distance will likely be shorter which can lead to higher coating porosity and lower density. The dissipation of heat may be reduced when coating an internal surface, meaning that substrate temperatures will increase further,

resulting in the greater oxidation of the splats post-impact. Due to these effects along with others, it cannot be predicted exactly how these coatings would perform if sprayed internally, although the data in this study indicate that the new HVOAF spray system used in this study is capable of spraying WC-Co-Cr coatings in line with other commercially used systems in terms of mechanical properties, so results are promising. The effects of spraying internally will be covered in future work.

In this study, it was shown that using the nanostructured powder did not increase microhardness as expected and due to having the worst mechanical properties of the three materials tested, the NC-30 coating will not be taken forward for future internal spray trials.

The results of this study show that while the MC-15 powder may be suitable for internal spraying due to the lower kinetic energy required and comparable performance to the conventional MC-30 powder in terms of the wear resistance and mechanical properties, the smaller powder particle size makes this material much more sensitive to temperature effects. These have been shown to impact the coating's microstructure and mechanical properties; however, when considering the shorter standoff distances often seen in internal diameter HVOF, this may be less of a significant issue.

Conclusion

Three WC-10%Co-4%Cr-based powders with varying powder particle size range and carbide grain sizes were deposited using a HVOAF system developed by Castolin Eutectic-Monitor Coatings Ltd. (UK). The microstructure of the powders and coatings were examined by SEM and XRD, followed by performance testing of the coatings by unlubricated sliding wear testing. From the results of this study, the following conclusions can be made:

- Characterization of the powder and coating microstructures using SEM and XRD revealed that the MC-15 powder decarburized during spraying to a greater extent compared to the MC-30 and NC-30 powders, possibly due to the finer powder reaching a higher temperature during spraying.
- The MC-15 and MC-30 coatings were found to have a similar microhardness, with the nanostructured coating possessing the lowest measured microhardness and fracture toughness. The reduction in fracture toughness may also be attributed to the relatively higher decarburization compared to MC-30 and NC-30.
- In the sliding wear testing at 96 N, the nanostructured coating performed best, making it the most suitable for low load applications. Oxidized particles that were observed on the surface of the MC-30 and MC-15 coatings at 96 N were not seen in the nanostructured coating, suggesting the formation of these oxidized particles is a key factor in the wear mechanism taking place. However, at 240 N this coating displayed the highest specific wear rates with the possible reason being its inferior microhardness and fracture toughness. Both the MC-30 and MC-15 coatings outperformed it by a similar degree; therefore, medium carbide coatings should be chosen for higher-load applications based on these data.
- For the development of a WC-Co-Cr coating for an internal spray application, the finer powder MC-15 is probably the most suitable due to the fact that the smaller size of this powder is a considerable advantage when spraying internally due to the lower kinetic energy required alongside comparable performance to the conventional MC-30 powder in terms of the wear resistance and mechanical properties. However, the smaller size of the powder leads to it being much more sensitive to temperature changes, meaning spray parameter optimization may be vital to reduce decarburization. Following the results of this study, the spray parameters used when applying coatings of the MC-15 powder with this ID HVOAF torch have been optimized further, with much lower decarburization and higher microhardness and fracture toughness being achieved.

Acknowledgments This work was supported by the Engineering and Physical Sciences Research Council [EP/L016362/1] in the form of an EngD studentship and industrial funding from Castolin Eutectic-Monitor Coatings Ltd.

References

1. M. Bielewski, *Replacing Cadmium and Chromium, the Research and Technology Organisation and NATO*, AG-AVT-140 (2011), Chp. 23, p 1/22
2. K. Legg and C. Pellerin, *SERDP/ESTCP Metal Finishing Workshop Summary*, SERDP & ESTCP Program Office, Washington, 2006
3. C. Lyphout and S. Björklund, Internal Diameter HVAF Spraying for Wear and Corrosion Applications, *J. Therm. Spray Technol.*, 2014, **24**, p 235-243
4. G. Bolelli, L. Berger, T. Börner, H. Koivuluoto, L. Lusvarghi, C. Lyphout et al., Tribology of HVOF- and HVAF-Sprayed WC-10Co4Cr Hardmetal Coatings: A Comparative Assessment, *Surf. Coat. Technol.*, 2015, **265**, p 125-144
5. L. Zhao, M. Maurer, F. Fischer, R. Dicks, and E. Lugscheider, Influence of Spray Parameters on the Particle In-Flight Properties

and the Properties of HVOF Coating of WC-CoCr, *Wear*, 2004, **257**(1-2), p 41-46
6. P. Chivavibul, M. Watanabe, S. Kuroda, J. Kawakita, M. Komatsu, K. Sato et al., Effect of Powder Characteristics on Properties of Warm-Sprayed WC-Co Coatings, *J. Therm. Spray Technol.*, 2009, **19**(1-2), p 81-88
7. L. Thakur and N. Arora, Sliding and Abrasive Wear Behavior of WC-CoCr Coatings with Different Carbide Sizes, *J. Mater. Eng. Perform.*, 2012, **22**(2), p 574-583
8. B. Kear, G. Skandan, and R. Sadangi, Factors Controlling Decarburization in HVOF Sprayed Nano-WC/Co Hardcoatings, *Scr. Mater.*, 2001, **44**(8-9), p 1703-1707
9. R. Schwetzke and H. Kreye, Microstructure and Properties of Tungsten Carbide Coatings Sprayed with Various High-Velocity Oxygen Fuel Spray Systems, *J. Therm. Spray Technol.*, 1999, **8**(3), p 433-439
10. B. Allcock, S. Gu, S. Kamnis, *Nozzle for a Thermal Spray Gun and Method of Thermal Spraying*. EP2411554A1, 2013
11. V. Katranidis, S. Gu, B. Allcock, and S. Kamnis, Experimental Study of High Velocity Oxy-Fuel Sprayed WC-17Co Coatings Applied on Complex Geometries. Part A: Influence of Kinematic Spray Parameters on Thickness, Porosity, Residual Stresses and Microhardness, *Surf. Coat. Technol.*, 2017, **311**, p 206-215
12. T. Sudaprasert, *An Investigation of Microstructure and Sliding Wear in Thermally Sprayed WC-Co Coatings*. Ph.D. The University of Nottingham, 2002
13. P. Shipway, D. McCartney, and T. Sudaprasert, Sliding Wear Behaviour of Conventional and Nanostructured HVOF Sprayed WC-Co Coatings, *Wear*, 2005, **259**(7-12), p 820-827
14. T. Sudaprasert, P. Shipway, and D. McCartney, Sliding Wear Behaviour of HVOF Sprayed WC-Co Coatings Deposited with Both Gas-Fuelled and Liquid-Fuelled Systems, *Wear*, 2003, **255**(7-12), p 943-949
15. P. Shipway, The Role of Test Conditions on the Microabrasive Wear Behaviour of Soda-Lime Glass, *Wear*, 1999, **233-235**, p 191-199
16. A.G. Evans and T.R. Wilshaw, Quasi-static Solid Particle Damage in Brittle Solids—I. Observations Analysis and Implications, *Acta Metall.*, 1976, **24**(10), p 939-956
17. J. Picas, E. Rupérez, M. Punset, and A. Forn, Influence of HVOF Spraying Parameters on the Corrosion Resistance of WC-CoCr Coatings in Strong Acidic Environment, *Surf. Coat. Technol.*, 2013, **225**, p 47-57
18. L. Jacobs, M. Hyland, and M. De Bonte, Comparative Study of WC-Cermet Coatings Sprayed via the HVOF and the HVAF Process, *J. Therm. Spray Technol.*, 1998, **7**(2), p 213-218
19. T. Gong, P. Yao, X. Zuo, Z. Zhang, Y. Xiao, L. Zhao, H. Zhou, M. Deng, Q. Wang, and A. Zhong, Influence of WC Carbide Particle Size on the Microstructure and Abrasive Wear Behavior of WC-10Co-4Cr Coatings for Aircraft Landing Gear, *Wear*, 2016, **362-363**, p 135-145
20. D. Stewart, P. Shipway, and D. McCartney, Abrasive Wear Behaviour of Conventional and Nanocomposite HVOF-Sprayed WC-Co Coatings, *Wear*, 1999, **225-229**, p 789-798
21. K. Jia and T.E. Fischer, Sliding Wear of Conventional and Nanostructured Cemented Carbides, *Wear*, 1997, **203-204**, p 310-318
22. E. Zakharova, I. Markova, A. Maslov, N. Polushin, and A. Laptev, Morphology of Powders of Tungsten Carbide Used in Wear-Resistant Coatings and Deposition on the PDC Drill Bits, *J. Phys. Conf. Ser.*, 2017, **857**, p 012058
23. S. Usmani, S. Sampath, D. Houck, and D. Lee, Effect of Carbide Grain Size on the Sliding and Abrasive Wear Behavior of Thermally Sprayed WC-Co Coatings, *Tribol. Trans.*, 1997, **40**(3), p 470-478
24. L. Jacobs, M. Hyland, and M. De Bonte, Study of the Influence of Microstructural Properties on the Sliding-Wear Behavior of HVOF and HVAF Sprayed WC-Cermet Coatings, *J. Therm. Spray Technol.*, 1999, **8**(1), p 125-132
25. H. Taimatsu, S. Sugiyama, and Y. Kodaira, Synthesis of W2C by Reactive Hot Pressing and Its Mechanical Properties, *Mater. Trans.*, 2008, **49**(6), p 1256-1261
26. J. Davis, *Handbook of Thermal Spray Technology*, ASM International, Materials Park, OH, 2004
27. G. Bolelli, L. Lusvarghi, and M. Barletta, HVOF-Sprayed WC-CoCr Coatings on Al Alloy: Effect of the Coating Thickness on the Tribological Properties, *Wear*, 2009, **267**(5-8), p 944-953
28. Y. Qiao, Y. Liu, and T. Fischer, Sliding and Abrasive Wear Resistance of Thermal-Sprayed WC-CO Coatings, *J. Therm. Spray Technol.*, 2001, **10**(1), p 118-125